Journal for ImmunoTherapy of Cancer

Optimal timing of anti-PD-1 antibody combined with chemotherapy administration in patients with NSCLC

Yachang Huo,[1] Dan Wang,[1] Shuangning Yang,[1,2] Yujie Xu,[3] Guohui Qin,[1] Chenhui Zhao,[1] Qingyang Lei,[1] Qitai Zhao,[1] Yaqing Liu,[1] Kaiyuan Guo,[1] Songyun Ouyang,[4] Ting Sun,[4] Hongmin Wang,[5] Feifei Fan,[5] Na Han,[6] Hong Liu,[5] Hongjie Chen,[5] Lijun Miao,[5] Li Liu ,[7] Yuqing Duan,[8] Wei Lv,[8] Lihua Liu ,[8] Zhixin Zhang,[9] Shundong Cang,[3] Liping Wang,[2] Yi Zhang [1,10,11,12,13]

To cite: Huo Y, Wang D, Yang S, *et al*. Optimal timing of anti-PD-1 antibody combined with chemotherapy administration in patients with NSCLC. *Journal for ImmunoTherapy of Cancer* 2024;**12**:e009627. doi:10.1136/jitc-2024-009627

► Additional supplemental material is published online only. To view, please visit the journal online (https://doi.org/10.1136/jitc-2024-009627).

YH, DW, SY and YX contributed equally.

Accepted 17 November 2024

For numbered affiliations see end of article.

Correspondence to
Professor Yi Zhang;
yizhang@zzu.edu.cn

Professor Liping Wang;
wlp@zzu.edu.cn

Dr Shundong Cang;
cangshundong@163.com

ABSTRACT

Background Anti-programmed cell death 1 (PD-1) antibody combined with chemotherapy simultaneously is regarded as the standard treatment for patients with advanced non-small cell lung cancer (NSCLC) by current clinical guidelines. Different immune statuses induced by chemotherapy considerably affect the synergistic effects of the chemo-anti-PD-1 combination. Therefore, it is necessary to determine the optimal timing of combination treatment administration.

Methods The dynamic immune status induced by chemotherapy was observed in paired peripheral blood samples of patients with NSCLC using flow cytometry and RNA sequencing. Ex vivo studies and metastatic lung carcinoma mouse models were used to evaluate immune activity and explore the optimal combination timing. A multicenter prospective clinical study of 170 patients with advanced NSCLC was performed to assess clinical responses, and systemic immunity was assessed using omics approaches.

Results PD-1 expression on $CD8^+$ T cells was downregulated on day 1 (D1) and D2, but recovered on D3 after chemotherapy administration, which is regulated by the calcium influx-P65 signaling pathway. Programmed cell death 1 ligand 1 expression in myeloid-derived suppressor cells was markedly reduced on D3. RNA sequencing analysis showed that T-cell function began to gradually recover on D3 rather than on D1. In addition, ex vivo and in vivo studies have shown that anti-PD-1 treatment on D3 after chemotherapy may enhance the antitumor response and considerably inhibit tumor growth. Finally, in clinical practice, a 3-day-delay sequential combination enhanced the objective response rate (ORR, 68%) and disease control rate (DCR, 98%) compared with the simultaneous combination (ORR=37%; DCR=81%), and prolonged progression-free survival to a greater extent than the simultaneous combination. The new T-cell receptor clones were effectively expanded, and $CD8^+$ T-cell activity was similarly recovered.

Conclusions A 3-day-delay sequential combination might increase antitumor responses and clinical benefits compared with the simultaneous combination.

WHAT IS ALREADY KNOWN ON THIS TOPIC

⇒ Chemotherapy combined with immune checkpoint blockade simultaneously has been widely used in patients with advanced non-small cell lung cancer (NSCLC); however, little is known about the optimal timing of combination treatment.

WHAT THIS STUDY ADDS

⇒ Our study showed that chemotherapy-induced programmed cell death 1 levels on $CD8^+$ T cells peaked on day 3 (D3) and declined in the subsequent 2 days in the paired peripheral blood of patients, which is regulated by the calcium influx-P65 signaling pathway. In the clinical practice of 124 matched patients with NSCLC, the sequential combination enhanced objective response rate, disease control rate, and progression-free survival to a greater extent than the simultaneous combination. The new T-cell receptor clones expanded, and $CD8^+$ T-cell activity was recovered.

HOW THIS STUDY MIGHT AFFECT RESEARCH, PRACTICE OR POLICY

⇒ Our study suggests that a 3-day-delay sequential combination might increase the clinical benefit compared with the simultaneous combination.

INTRODUCTION

Immune checkpoint blockade of programmed cell death 1 (PD-1) and programmed cell death 1 ligand 1 (PD-L1) leads to an effective immune response in various malignant tumors.[1] Clinical studies have shown notable improvements in overall survival without an increase in adverse events in patients receiving chemotherapy combined with immunotherapy.[2] For patients with advanced non-small cell lung cancer (NSCLC) without sensitive gene mutations, platinum-based chemotherapy combined with anti-PD-1 antibody has been recommended as the first-line treatment according to the National Comprehensive Cancer Network guidelines.[3] However, some patients do not benefit from the combined therapy.[4]

Different chemo-anti-PD-1 combination strategies have shown different antitumor effects.[5] Therefore, it is necessary to explore the optimal combination strategies.

Based on the clinical guidelines for NSCLC, chemotherapy combined with anti-PD-1 antibodies has been widely applied in current clinical practice.[3 6] Unfortunately, there is still no thorough research on diverse combinations of chemotherapy and anti-PD-1 antibodies. In preclinical animal trials, anti-PD-1 antibody administered 3 days after oxaliplatin therapy considerably suppressed tumor development compared with oxaliplatin and anti-PD-1 antibody used simultaneously.[7] Compared with the simultaneous combination, the anti-PD-1 antibody administered 1 day after cisplatin therapy dramatically enhanced the antitumor immune response.[8] Based on these findings, administration of chemotherapy before immunotherapy may maximize the synergistic anticancer effects of chemo-anti-PD-1 therapy. In clinical trials of neoadjuvant chemo-anti-PD-1 therapy for patients with esophageal cancer, participants treated with anti-PD-1 antibody 2 days after chemotherapy exhibited a greater percentage of pathological complete remission (36%) than those treated with the simultaneous combined regimen (7%).[9] These results suggest that chemotherapy simultaneously combined with anti-PD-1 antibody may not be the optimal combination strategy. Various combination timings may produce varied clinical effects[9 10]; therefore, pertinent studies require comprehensive mechanistic research and the stringent verification of evidence-based medicine. Furthermore, exploring the optimal combination timing of chemotherapy-anti-PD-1 may be conducive to improving the clinical outcomes of patients with NSCLC.

Anti-PD-1 therapy inhibits tumor progression by activating the antitumor immune response.[11 12] The beneficial immune response to anti-PD-1 antibody is closely associated with the cytotoxic effects of activated $CD8^+$ T cells and high PD-1 expression.[11 13 14] Chemotherapy has different immunomodulatory effects in killing tumor cells. Chemotherapeutic drugs such as cisplatin lead to immunogenic tumor cell death, contributing to the activation of tumor antigen-specific $CD8^+$ T cells.[15 16] Our previous study identified the regulation of PD-1 on T cells via the danger signaling molecule, high-mobility group protein B1.[17] A recent preclinical study revealed that platinum notably impaired the proliferation of activated lymphocytes.[10] In the acute inflammation model, PD-1 expression on $CD8^+$ T cells initially increased and subsequently decreased, which was comparable to the antigen generation induced by chemotherapy.[18] These results indicate that chemotherapy may trigger immunosuppressive or immune-activated responses at different times, thereby affecting the clinical efficacy of chemo-anti-PD-1 therapy. Thus, it is crucial to thoroughly analyze the dynamic changes in immune activity after chemotherapy.

In our study, dynamic changes in immune status induced by platinum-based chemotherapy alone in patients and a preclinical model were investigated. We analyzed the PD-1 expression at different time points after chemotherapy, which is mainly associated with the efficacy of PD-1 blockade, and explored the underlying mechanism. Ex vivo and in vivo studies were performed to determine optimal combination timing. Furthermore, to ensure that the optimal combination timing was suitable for clinical patients, a multicenter prospective clinical study was performed on 170 patients with advanced NSCLC, and underlying alterations in systemic immunity were analyzed using omics approaches. These findings highlight that optimal combination timing can improve the synergistic antitumor response.

METHODS

Study design and assessment

199 patients pathologically diagnosed with NSCLC between January 2021 and May 2023 were included in this study, including those who received chemotherapy only (n=29) and those who received chemo-anti-PD-1 combination therapy (n=170). Patients with NSCLC aged 18–79 years were eligible for enrollment. The key eligibility criteria for all patients included an Eastern Cooperative Oncology Group performance status score of 0–1, adequate organ function, and the presence of at least one measurable lesion, according to the Response Evaluation Criteria in Solid Tumors (RECIST) V.1.1. Key exclusion criteria included a history of bone marrow or solid organ transplantation; ongoing or recent autoimmune disease requiring systemic immunosuppressive therapy; history of severe hypersensitivity reactions to any monoclonal antibody, gemcitabine, pemetrexed, paclitaxel, and platinum; and previous monoclonal antibody treatment targeting PD-1/PD-L1/cytotoxic T-lymphocyte associated protein 4 (CTLA-4).

The patients who received chemotherapy alone (n=29) were treated with platinum-based chemotherapy. In addition to platinum-based agents, the regimen included docetaxel, paclitaxel, or pemetrexed. Blood samples were collected during the platinum-based treatment cycle.

Patients who received chemo-anti-PD-1 combination therapy (n=170) from five hospitals were separated into two cohorts and their clinical responses were evaluated in a multicenter prospective observational clinical study. One cohort (n=102) was treated with anti-PD-1 antibody on the first day of platinum-based chemotherapy (simultaneous combination). The other cohort (n=68) was administered anti-PD-1 antibody on the third day after the end of chemotherapy (3-day delayed sequential combination). PD-L1 high was defined as the presence of membrane staining of any intensity in ≥50% of tumor and immune cells. The primary endpoint was the objective response. The key secondary endpoints were disease control rate, clinical benefit rate, and safety. The clinical response was assessed for each target lesion based on RECIST (V.1.1) every two cycles. Adverse events were recorded according to the Common Terminology Criteria for Adverse Events V.5.0. Adverse events were recorded for all treated patients until 3 months after

the administration of the last anti-PD-1 antibody dose or death.

This study was conducted in accordance with the Strengthening the Reporting of Observational Studies in Epidemiology reporting guideline for observational studies.

Associations of clinicopathological parameters with simultaneous combination and 3-day delayed sequential combination were estimated with modified Poisson regression (simultaneous combination, 3-day delayed sequential combination). The propensity score matching scores were calculated using logistic regression, taking into account several demographic and clinical characteristics. We performed 1:1 "greedy nearest-neighbor" matching without replacement with a caliper of 0.15. The method functionally relied on the R package MatchIt. Treatment efficacy was performed comparisons for both pre-matching and post-matching data to evaluate the validity of our results. For objective response rate, a stratified Cochran-Mantel-Haenszel test was used to calculate common ORs and associated two-sided 95% CIs. A stratified Cox proportional hazards model was used to estimate the treatment effect HR. Furthermore, sensitivity analyses were conducted to assess the validity of our results and investigate plausible variables that may have impacted the noted variations in treatment efficacy between the two cohorts.

Mice

Female C57BL/6 mice (16–18 g, 4–6 weeks old) were obtained from the animal facility (Beijing Vital River Laboratory Animal Technology) and were fed in the Animal Experiment Center of Henan Province.

Mice model

We injected 1×10^6 luciferase-labeled *Luc-GFP-LLC* cells into the tail vein and monitored lung metastases. For in vivo determination of the metastatic burden, mice were anesthetized and injected intraperitoneally with 75 mg/kg D-luciferin (100 mL of 30 mg/mL in phosphate-buffered saline (PBS)) 10 min before imaging. Metastatic growth was monitored over time using an IVIS Spectrum Imaging System (PerkinElmer) and analyzed using the coupled Living Image software program (PerkinElmer).

For chemotherapy experiments, once tumors reached the total thorax bioluminescence imaging (BLI) signal of $1e^5$–$1e^7$, the mice were randomly assigned to the experimental groups. All the mice were intraperitoneally injected with a single dose of cisplatin (10 mg/kg) and pemetrexed (100 mg/kg).

For combination therapy experiments, once tumors reached the total thorax BLI signal of $1e^5$–$1e^7$, the mice were randomly assigned to the experimental groups. Cisplatin (10 mg/kg), pemetrexed (100 mg/kg), NaCl 0.9%, anti-PD-1 antibody (200 mg/mouse, BE0273, Bio X Cell), or IgG2a isotype (200 mg/mouse, BE0089, Bio X Cell) was administered via intraperitoneal injection once after randomization.

Tissue digestion and preparation of single-cell suspensions

Single-cell suspensions of tumor tissues and spleens were prepared on scheduled days after treatment. For tumor-infiltrating lymphocytes isolation, tumors were excised, manually dissociated and digested in collagenase/DNase mix (Roche) for 30 min at 37°C. The cells collected from each mouse were resuspended in an equal volume of fluorescence-activated cell sorting buffer for flow cytometry. When chemotherapy samples were treated with the PD-1 monoclonal antibody in vitro, 1×10^6 cells were plated in a 24-well plate, and PD-1 monoclonal antibody (10 mg/mL, Camrelizumab, Hengrui) was added 24 hours before flow cytometry antibody staining.

Surface and intracellular staining and flow cytometry

Up to 2×10^6 dissociated cells were resuspended in Zombie Aqua Dye (B324732, BioLegend) viability dye solution (1:500 in PBS), followed by 15 min of incubation at room temperature in the dark. Cells were then centrifuged, resuspended in FACS buffer, and stained at $0.5–1\times10^6$ cells/mL concentration. Surface staining was performed with antibody for 30 min at 4°C in FACS buffer using the antibodies listed in online supplemental table 6. Following incubation, the cells were washed twice with PBS before intracellular staining. For intranuclear staining, cells were first stained on the surface before fixation (G1101, Servicebio) and for interferon (IFN)-γ, interleukin (IL)-2, marker of proliferation Kiel 67 (Ki-67), Thymocyte Selection Associated High Mobility Group Box (TOX) and T-cell factor 1 (TCF1) was performed with Foxp3 Staining Buffer Set (eBioscience) according to manufacturer's instruction, followed by intranuclear staining. All data were acquired using a Beckman Coulter DxFLEX flow cytometer equipped with CytExpert experiment-based software (Beckman Coulter), and data were analyzed using FlowJo software (Tree Star) or CytExpert.

Intracellular Ca^{2+} measurement

Cells were incubated in Hank's Balanced Salt Solution (HBSS) containing 4 mM Fluo-4 AM (Beyotime) for 45 min and washed three times with HBSS. Then they were stained with CD8 surface antibody and rinsed three more times with HBSS. At the end of the staining, 60 s were first recorded by flow cytometry as a baseline, and then the calcium flow variation was recorded for 2 min by flow cytometry immediately after extracellular stimulation with the addition of 25 µg/mL anti-CD3 mAbs (317326, BioLegend).

Immunofluorescence

$CD8^+$ T cells were sorted from peripheral blood mononuclear cell (PBMC) of chemotherapy patients. The cells were applied to slides at a concentration of 10^3/µL, allowed to dry and then immediately fixed with 4% paraformaldehyde for 20 min, permeabilized with 1% Triton X-100 for 15 min, and sealed at room temperature. Then, the cells were incubated with primary antibodies

Phospho-NF-κB p65 (Ser536) (93H1) Rabbit mAb (3033T, CST, 1:500), PD-1/CD279 mAb (66 220–1-Ig, Proteintech, 1:500) overnight at 4°C, and then rewarmed at room temperature for 1 hour the next day. The cells were washed three times with PBS, and then incubated with Alexa Fluor 488-AffiniPure Donkey Anti-Mouse IgG (715-545-150, Jackson)/Alexa Fluor 594-AffiniPure Donkey Anti-Rabbit IgG (711-585-152, Jackson) for 1 hour and washed three times with PBS. An appropriate amount of anti-fluorescence quenching sealing solution (containing 4',6-diamidino-2-phenylindole, DAPI) (P0131-25 mL) was added, coverslips were covered, and 15 min were observed and imaged by Vectra imaging system with excitation wavelengths of 405 and 488 nm and 594 nm.

RNA sequencing and analysis

Frozen PBMC samples from four chemotherapy patients, collected on D0, D1, and D3 (except one patient whose PBMC sample was not collected on D1), and that of six patients (three from each combination group), collected on D0 and D7, were purified with $CD8^+$ T magnetic beads (130-045-201, Miltenyi Biotec) using magnetic-activated cell sorting columns (130-042-401, Miltenyi Biotec). RNA sequencing and data analysis were performed using BGI 500 (Wuhan, China). Differential expression analysis was performed using DEGseq with fold changes ≥2 and Q value ≤0.05 in the chemotherapy group, while using DESeq2 (V.1.4.5) with fold changes ≥2 and Q value ≤0.05 in the combination group.

T-cell receptor sequencing

T-cell receptor (TCR) sequencing of pretreatment and post-treatment blood samples was performed to assess the new clones and the correlation of changes with the response using immune sequence analysis at Chengdu ExAb Biotechnology. A total of 30,000 functional TCR sequences were randomly selected from each sample for comparison.

Statistical analysis

Prism (GraphPad Software V.8.0.1) or Statistical Product Service Solutions V.21, if applicable, were used to produce all summary statistics (average values, SD, SEM, and significant differences between groups). Unpaired (for mouse and human non-longitudinal samples) or paired (for human longitudinal samples) two-tailed Student's t-tests were used to evaluate the statistical significance between groups ($p<0.05$, considered statistically significant). The log-rank (Mantel-Cox) test was used to compare survival across multiple groups using the Prism software.

RESULTS

The dynamic changes of circulating immune cells induced by chemotherapy in NSCLC

Accumulating evidence has shown a potentially significant role for systemic $CD8^+$ T cells in the response to anti-PD-1 antibodies.[12 14 19 20] High PD-1 expression on circulating $CD8^+$ T cells or an increased ratio of PD-1 expression on $CD8^+$ T cells to that on $CD4^+$ T cells contributes to a beneficial response to PD-1 blockade.[21–23] Enhanced expression of systemic CD8-PD-1 signaling was observed in the responders (online supplemental figure 1A). Thus, we further validated that $CD8^+$T cells with PD-1 expression in the peripheral immune system have the ability to respond to PD-1 monotherapy and that PD-1 hyper-expression with superior performance after checkpoint blockade. Indeed, these patients demonstrated improved progression-free survival (PFS) after the checkpoint blockade (online supplemental figure 1B). The external breast cancer combination therapy cohort confirmed that PD-1 hyper-expression on circulating $CD8^+$ T cells was positively associated with long-term PFS[24] (online supplemental figure 1C).

To profile the dynamic changes of the circulating immune status regulated by platinum-based chemotherapy, PBMC from patients with NSCLC (n=29) before day 0 (D0) and after (D1, D2, D3, D5, and D7) chemotherapy administration were collected (figure 1A). Flow cytometry was performed, and the results showed that PD-1 expression on $CD8^+$ T cells was downregulated on D1 and D2, recovered or even higher on D3, and then declined to basal levels on D5 and D7 (figure 1B and online supplemental figure 2A). Similarly, noteworthy peak values were detected for the ratio of PD-1 expression on $CD8^+$ T cells to that on $CD4^+$ T cells on D3 (figure 1C and online supplemental figure 2B). Meanwhile, the expression of PD-L1 on monocytic myeloid-derived suppressor cells (M-MDSCs) and the proportion of M-MDSCs in PBMC were at a trough on D3 (figure 1D,F, online supplemental figure 2C,D). PD-L1 expression on polymorphonuclear MDSC (PMN-MDSCs) was also the lowest on D3 (figure 1E). The PMN-MDSC ratio in myeloid cells decreased at the end of the treatment (figure 1F). Moreover, the ratio of central memory (CM) and effector (eff) T cells (T_{CM}/T_{eff}), which reached a maximum on D3 (online supplemental figure 2E), was associated with an improved prognosis.[25] CD28, a vital molecule activated on T cells, reached its highest expression on D3 (figure 1G, online supplemental figure 2F). Transcription factor TCF1 is an essential transcription factor in progenitor-exhausted $CD8^+$ T cells.[26 27] There was a consistent peak in the $TCF1^+PD\text{-}1^+CD8^+$ T cell subset with CD28 expression (figure 1H).

To further identify immune cell alterations elicited by chemotherapy in vivo, we injected Luc-LLC cells into the tail vein and treated tumor-bearing mice with cisplatin and pemetrexed (figure 1I). Tumor tissues and spleens were collected from the mice before (D0) or after chemotherapy treatment (D1, D3, D5, and D7). The proportion of $CD8^+PD\text{-}1^+$ T cells in the spleen and tumor tissues peaked on D3 and then gradually decreased, whereas the expression of PD-L1 on MDSC showed the opposite trend (figure 1J,K), which was consistent with the patient with NSCLC results. The ratio of PD-1 expression on circulating $CD8^+$ T cells to that on $CD4^+$ T cells peaked on D3

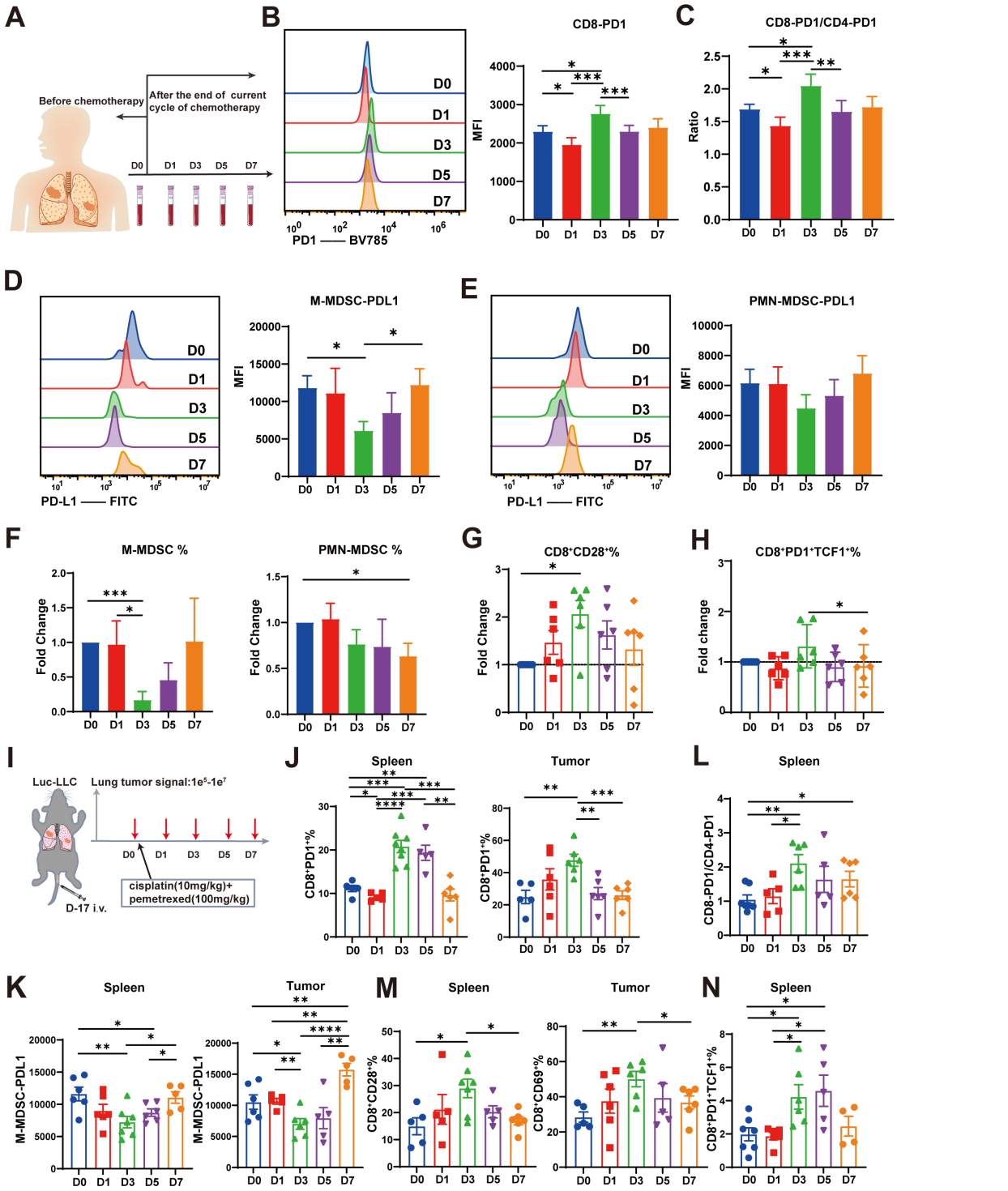

Figure 1 The dynamic changes of circulating immune cells induced by chemotherapy in NSCLC. (A) Strategy for blood sample collection from patients with NSCLC for analysis. (B) The PD-1 expression on $CD8^+$ T cells was detected in paired pre-chemotherapy (D0) and post-chemotherapy (D1, D3, D5, D7) PBMC using flow cytometry. (C) The ratio of PD-1 expression on $CD8^+$ T cells to that on $CD4^+$ T cells. (D–E) The PD-L1 expression on M-MDSC (D) and PMN-MDSC (E) from chemotherapy patients. (F) Proportion of M-MDSC and PMN-MDSC in myeloid cells. (G, H) Frequency of $CD28^+$ (G) and $TCF1^+$ (H) cells among the total $CD8^+$ T cells. (I) Schematic schedule of tail vein tumor injection, cisplatin plus pemetrexed therapy dosing and tumor sampling (J) Frequency of PD-1^+ cells in the $CD8^+$ population in spleen and tumor of five groups. (K) Cell surface levels of PD-L1 in M-MDSCs and PMN-MDSCs. (L) The ratio of PD-1 expression on $CD8^+$ T cells to that on $CD4^+$ T cells in the spleen. (M) Frequency of $CD28^+$ (in spleen) and $CD69^+$ (in tumor) in total $CD8^+$ T cells. (N) Frequency of $TCF1^+PD\text{-}1^+$ cells in total $CD8^+$ T cells in the spleen. (A–N) Mean±SEMs. Pairwise comparisons were also performed. P value, Student's t-test. *p<0.05, **p<0.01, ***p<0.001. B–C, n=11. D–F, n=8. G–H, n=6. i.v., intravenous; M-MDSC, monocytic myeloid-derived suppressor cell; MFI, mean fluorescent intensity; NSCLC, non-small cell lung cancer; PD-1, programmed cell death 1; PD-L1, programmed cell death 1 ligand 1; PMN-MDSC, polymorphonuclear MDSC; TCF1, T-cell factor 1.

as well (figure 1L). The expression of activated markers, CD28 and CD69, on $CD8^+$ T cells rapidly increased on D3 (figure 1M). A similar rise was observed in circulating progenitor-exhausted $CD8^+$ T cells ($TCF1^+PD\text{-}1^+CD8^+$ T cells) (figure 1N). Thus, our in vivo study verified the results observed in patients with NSCLC and demonstrated that D3 was the optimal immune status for chemo-anti-PD-1 combination therapy.

Moreover, $CD8^+$ T-cell apoptosis increased abruptly on D1 and D2 after chemotherapy administration and then decreased on D3 (online supplemental figure 2G). The absolute number of $CD8^+$ T cells showed first fall and then rise (online supplemental figure 2H). Furthermore, in vitro studies showed that chemotherapy simultaneously combined with a PD-1 antibody enhanced $CD8^+$ T apoptosis more than chemotherapy alone (online supplemental figure 2I). These results demonstrated that the simultaneous combination might enhance $CD8^+$ T-cell apoptosis, and the anti-PD-1 therapy on D3 after chemotherapy might avoid the toxicity of chemotherapy. Overall, these data indicate that D3 after chemotherapy is the time frame with the optimal immune status for patients with NSCLC who benefited from chemo-anti-PD-1 combination therapy.

Gene expression profile of circulating $CD8^+$ T cells from patients with NSCLC after chemotherapy

$CD8^+$ T cells purified before (D0) and after (D1 and D3) chemotherapy were used for RNA sequencing (RNA-seq). Volcano plot analysis revealed differentially expressed genes between the D0 and D3 groups (figure 2A). Gene Ontology analysis showed that the upregulated genes on D3 were mainly enriched in the cell adhesion, migration, and chemotaxis pathways (figure 2B). *TCF7* and *CD28* expression increased, while that of the exhausted molecule (*TOX*) decreased on D3 compared with that on D0 or D1 (figure 2C). A recent study reported a group of genes that drive T-cell proliferation and activation, including *MAPK3*, a critical mediator of T-cell functions, the co-stimulatory molecule *CD59*, the transcription factor *BATF*, and cytokines, which are known to promote T-cell proliferation, such as *IL-12B* and *IL-23A*.[28] In our data set, these genes were upregulated on D3 (figure 2C). To further investigate temporal changes in the transcription of $CD8^+$ T cells, we applied a soft clustering approach using Mfuzz, which groups genes based on their expression profiles. We identified six time-dependent expression patterns (figure 2D) and investigated their biological significance. Cluster 2 contained 199 genes and cluster 6 contained 152 genes enriched in immune and inflammatory responses. Serious damage was detected on D1, with full or partial recovery of $CD8^+$ T cells function observed on D3 during systemic chemotherapy. Cluster 1 contained 240 genes, and cluster 5 contained 248 genes related to cell migration and cell adhesion, which showed increased expression levels over time (figure 2D). Additionally, we performed Gene Set Enrichment Analysis (GSEA) using established signatures of $CD8^+$ T cells with PD-1 high expression in humans. A memory phenotype distinct from exhausted $CD8^+$ T cells was represented in this instance by the gene signature, which was enriched in the D3-subsets (figure 2E). In summary, T cells on D3 are in the initial phase, in which functionality begins to gradually recover rather than becoming anergic or terminally exhausted.

PD-1 on $CD8^+$ T cells highly expressed on D3 was regulated by calcium influx-P65 activation after chemotherapy

The dynamic expression of PD-1 on $CD8^+$ T cells after chemotherapy is a key factor in determining the timing of PD-1 antibody treatment. The above results suggest that PD-1 reached its highest expression on D3, however, the underlying mechanism remains unclear. We analyzed the RNA-seq data of $CD8^+$ T cells purified before (D0) and after chemotherapy (D1 and D3), and found that calcium inward flow-related pathways were upregulated in $CD8^+$ T cells from D3 (figure 3A). Transcription factor enrichment analysis of genes elevated in the D3 group relative to the D0 or D1 groups predicted that RELA was a core transcription factor regulating more other genes (figure 3B). Furthermore, we validated that calcium flux in $CD8^+$T cells was upregulated on D3, and then declined to basal levels in D5 and D7 from patients with NSCLC treated with chemotherapy administration alone by flow cytometry (figure 3C,D). The expression of phosphorylated P65 in $CD8^+$ T cells was consistent with calcium flux, peaking at D3 (figure 3E). Immunofluorescence imaging showed that chemotherapy-induced P65 activation and nuclear translocation in $CD8^+$ T cells on D3, and the fluorescence intensity of PD-1 was upregulated on D3 (figure 3F). The calcium chelator BAPTA and NF-κB inhibitor QNZ significantly inhibited P65 activation and PD-1 expression on D3, and the inhibition ratio was greater than that at other times (figure 3G,H). These findings indicate that PD-1 on $CD8^+$T cells highly expressed on D3, is mainly regulated by calcium influx-P65 activation after chemotherapy.

Anti-PD-1 antibody treatment influences the function of $CD8^+$ T cells at different times after chemotherapy ex vivo

To determine the best response to anti-PD-1 antibody, we collected PBMC from patients with NSCLC before and after chemotherapy and treated them with anti-PD-1 antibody at different time points (D0, D1, D2, D3, D5, and D7). CD28 expression on $CD8^+$ T cells was enhanced on D3 (figure 4A, online supplemental figure 3A). The percentage of $TCF1^+PD\text{-}1^+CD8^+$ T cells was not significantly different on the different days (figure 4B and online supplemental figure 3B). TOX expression in $CD8^+$ T cells remained low after chemotherapy compared with that on D0 (figure 4C, online supplemental figure 3C). Next, we evaluated

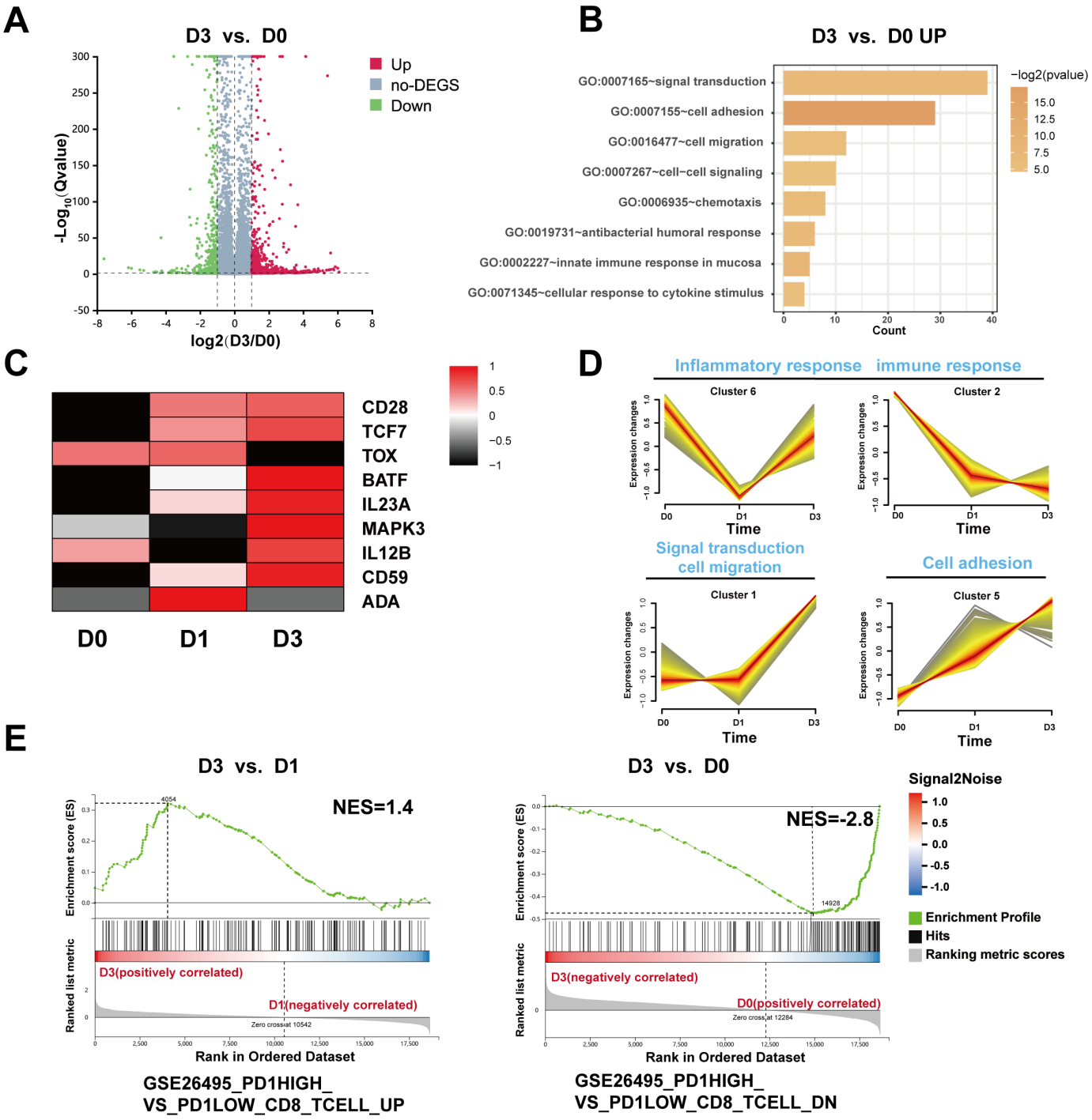

Figure 2 Gene expression profile of circulating CD8$^+$ T cells from patients with non-small cell lung cancer receiving chemotherapy. (A) Volcano map of differentially expressed genes between D3 and D0. (B) The top eight biological processes associated with immunity enriched by Gene Ontology analysis performed on the upregulated genes in D3 CD8$^+$ T cells compared with D0 CD8$^+$ T cells. Bar graph colored by p values. (C) Heatmap showing transcriptome relative expression of function-related molecules. (D) Clusters showing key biological processes terms. Genes clustered by their expression pattern along the progression of therapy by the Mfuzz R package. (E) Gene Set Enrichment Analysis of programmed cell death 1 high CD8$^+$ T cells; D3 CD8$^+$ T cells had elevated gene expression signatures compared with D1 or D0 CD8$^+$ T cells. NES, normalized enrichment score.

the activated function of CD8$^+$ T cells. The proportion of IFN-γ^+, and Ki67$^+$ cells were noticeably increased in D3 PBMC after PD-1 blockade (figure 4D, online supplemental figure 3D). Furthermore, the cytotoxic function and proliferation of CD8$^+$PD-1$^+$ T cells, which are considered to be highly enriched in antigen-specific T cells,[29] showed a trend similar to that of CD8$^+$ T cells (figure 4E, online supplemental figure 3E). Therefore, evidence suggests that the application of PD-1 blockade on D3 after

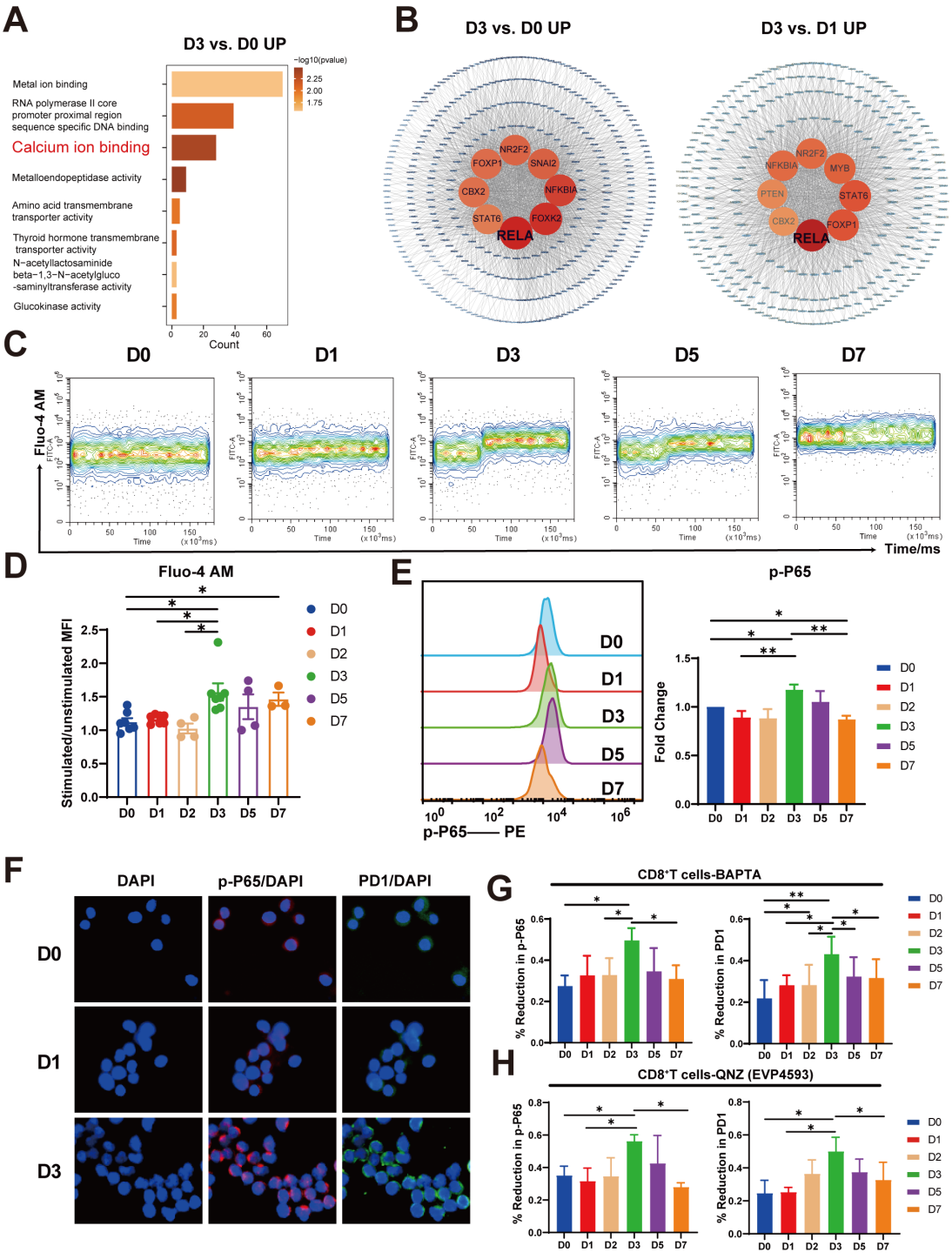

Figure 3 The high expression of PD-1 on CD8⁺T cells was regulated by calcium influx-P65 signaling on D3 after chemotherapy. (A) The top eight molecular function enriched by Gene Ontology analysis performed on the upregulated genes in D3 CD8⁺T cells compared with D0 CD8⁺T cells. Bar graph colored by p values. (B) The network was visualized with Cytoscape V.3.10.1. The transcription factor with the highest ranking is shown by the central circle, and its association with more genes is indicated by a darker red color. Transcription factor of genes elevated in the D3 group were predicted using the KnockTF2.0 database. (C–D) Fluo-4 AM MFI of cytosolic calcium release in CD8⁺ T cells from paired pre-chemotherapy (D0) and post-chemotherapy (D1, D2, D2, D5, D7) PBMC using flow cytometry. Data are representative of seven independent experiments (C). Quantification of MFI is shown (D, n=7). (E) The p-P65 expression on CD8⁺T cells was detected in PBMC from patients receiving chemotherapy (n=8). (F) Immunofluorescence staining of PD-1 (green) and p-P65 (red) in CD8⁺ T cells. Nuclei were stained with DAPI. (G–H) PBMC from patients receiving chemotherapy were pretreated with BAPTA (MCE, HY-100168, G, 10 mM, n=5) or the NF-κB inhibitor QNZ (Selleck, S4902, H, 10 nM, n=4) for 24 hours and flow cytometry-based quantification of p-P65 and PD-1 (expressed as MFI) were analyzed. (D–H) Mean±SEMs. *p<0.05, **p<0.01, ***p<0.001. DAPI, 4',6-diamidino-2-phenylindole; MFI, mean fluorescent intensity; PBMC, peripheral blood mononuclear cell; PD-1, programmed cell death 1; p-P65, phosphorylated P65.

chemotherapy remarkably restores the anti-tumor activity of CD8$^+$ T cells.

Prolonged survival of mice treated with anti-PD-1 antibody on D3 after chemotherapy

To further verify the optimal timing for chemo-anti-PD-1 combination therapy, we tested the anti-tumor effects of chemo-anti-PD-1 combined with sequencing in a mouse model of metastatic lung carcinoma. 17 days after Luc-LLC inoculation, the tumor-bearing mice were randomized and separated into six groups for different treatments. Anti-PD-1 therapy initiated simultaneously with chemotherapy ((Cis+Pem+αPD-1(D0)) showed synergy in the inhibition of tumor growth and increased survival compared with chemotherapy (Cis+Pem) or anti-PD-1 antibody treatment alone (figure 5A–D). A 3-day-delay PD-1 blockade after chemotherapy ((Cis+Pem+αPD-1(D3)) fully reinforced the anti-tumor effects more than the other combined treatment strategies ((Cis+Pem+αPD-1(D0, D7)) (figure 5A–D). Importantly, the Cis+Pem+αPD-1(D3) (median survival, reached at 66 days) trended (p=0.019) toward a greater survival benefit than the regimen of Cis+Pem+αPD-1(D0) (median survival of

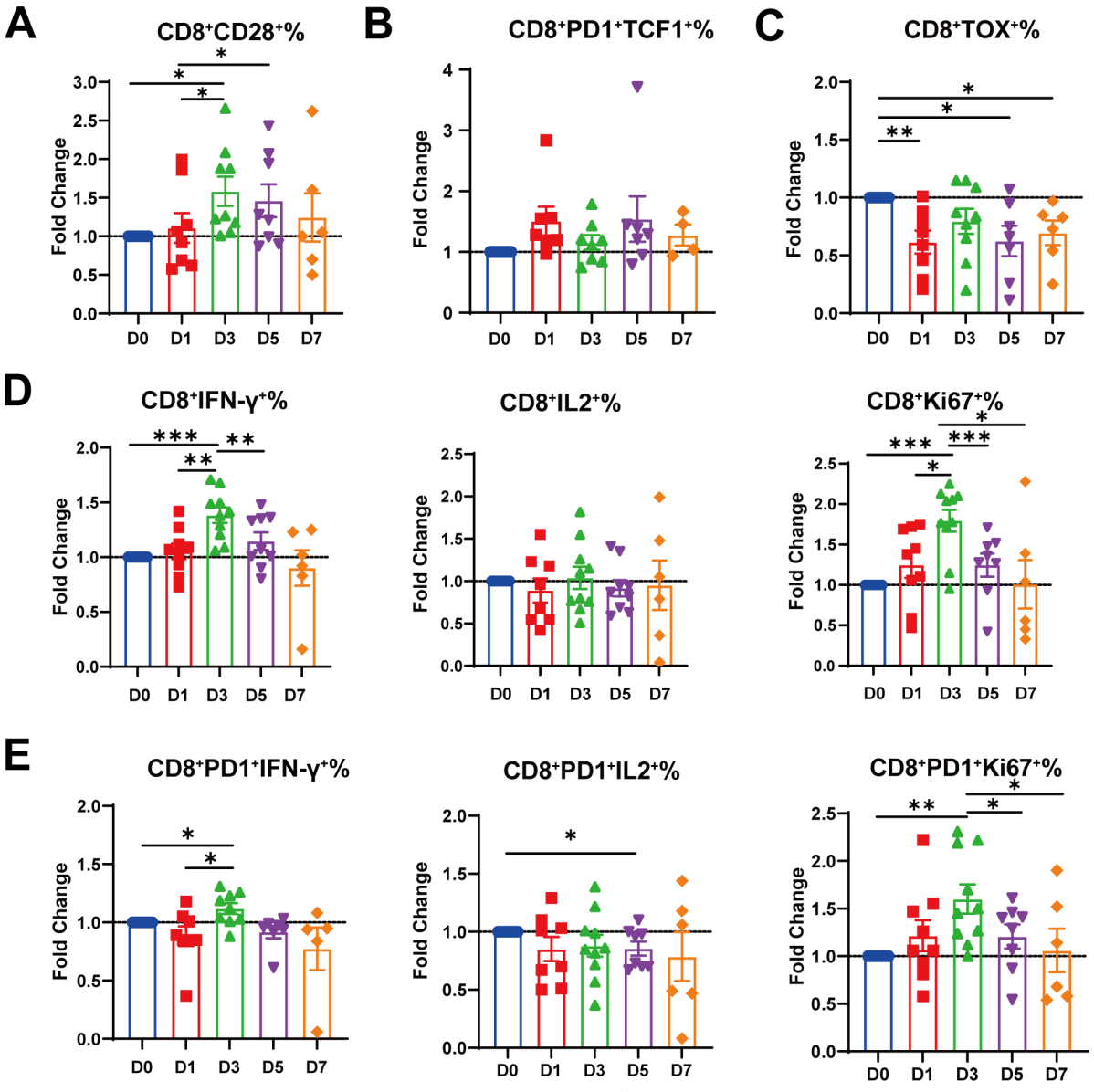

Figure 4 Anti-PD-1 antibody treatment influences the function of CD8$^+$ T cells at different times after chemotherapy ex vivo. (A, C) D0, D1, D3, D5, and D7 peripheral blood mononuclear cells from patients receiving chemotherapy were treated with anti-PD-1 antibody (10 mg/mL) for 24 hours. Flow cytometry was used to examine the frequency of CD28$^+$ (A) and TOX$^+$ (C) cells among the total CD8$^+$ T cells. (B) Frequency of TCF1$^+$ cells in total CD8$^+$ PD-1$^+$ T cells. (D–E) Frequency of IFN-γ$^+$, IL-2$^+$, Ki67$^+$ cells in total CD8$^+$ T cells (D) and total CD8$^+$PD-1$^+$ T cells (E). A–E Mean±SEMs *p<0.05, **p<0.01, ***p<0.001 A, C, n=9. B, n=8. D–E, n=10. IFN, interferon; IL, interleukin; Ki-67, marker of proliferation Kiel 67; PD-1, programmed cell death 1; TCF1, T-cell factor 1; TOX, Thymocyte Selection Associated High Mobility Group Box.

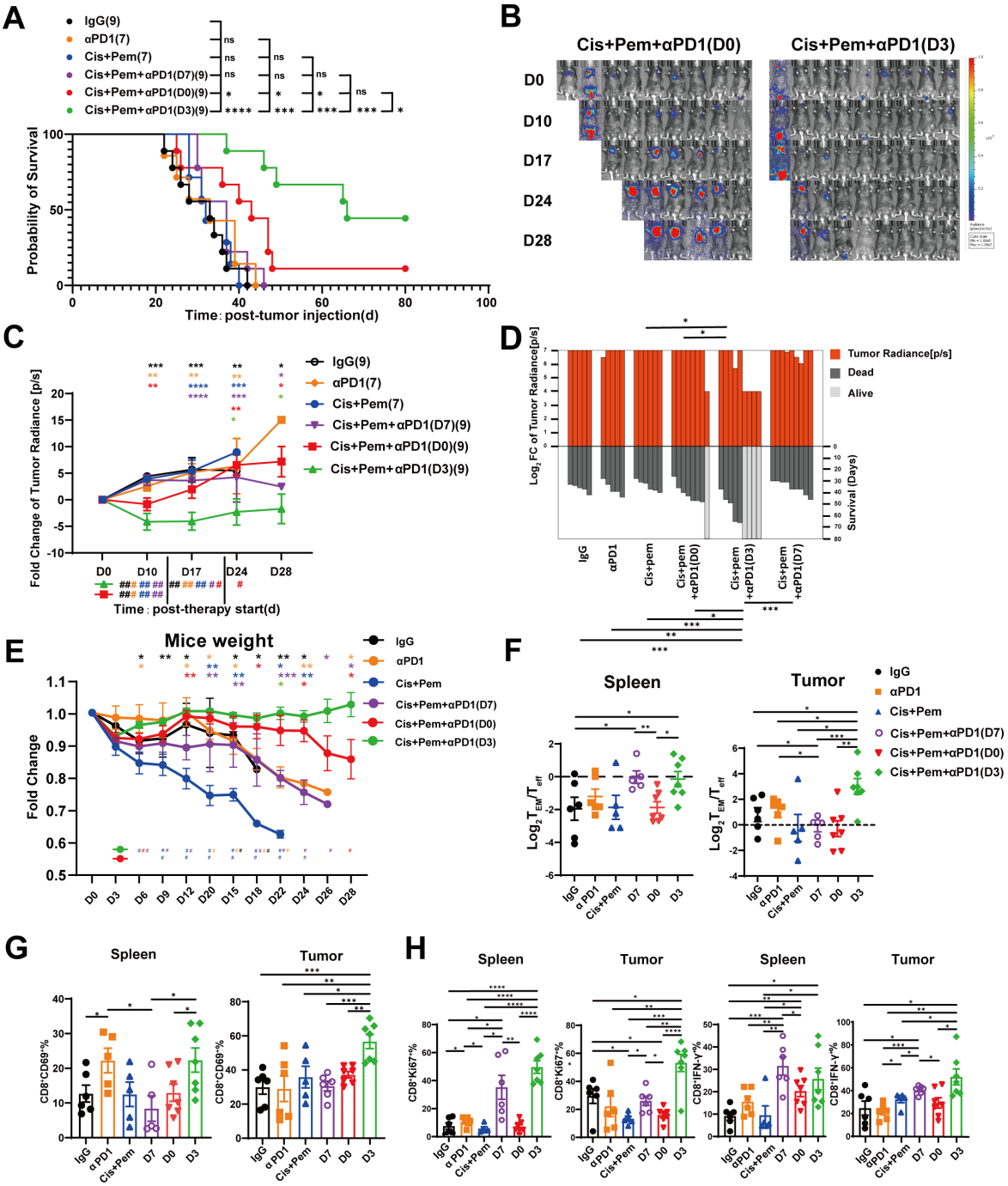

Figure 5 Mice treated with anti-PD-1 antibody 3 days after chemotherapy had considerably prolonged survival. (A) Survival of mice administered chemotherapy and anti-PD-1 antibody alone or in combination at different time points. *p<0.05, **p<0.01, ***p<0.001. ns, not significant (log-rank test). (B) In vivo BLI of lung metastasis developed after intravenous injection of Luc-LLC cells. Representative images in the focused treatment group are shown, D0 refers to the day of treatment. (C) Temporal BLI quantification (radiance, photons/s) based on the dosing timeline in thorax tumor burden. Data is mean±SEM based on the indicated numbers of mice in various regimen groups. Pairwise comparisons of the group (Cis+Pem + αPD-1(D0)), (Cis+Pem + αPD-1(D3)) versus the other group at different time points denoted by the specific color of symbol#. #p<0.05, ##p<0.01. *Indicates death of mice, resulting in reduced mean BLI values. (D) SK plots included tumor burden and survival data after various treatments until death or observation endpoint. For ease of observation, we set the maximum radiance fold change value to 7. *p<0.05, **p<0.01, ***p<0.001 (E) mice weight based on the timeline. Data is mean±SEM based on the indicated numbers of mice in various regimen groups. Pairwise comparisons of the group (Cis+Pem + αPD-1(D0), (Cis+Pem + αPD-1(D3)) versus the other group denoted by the specific color of symbol #. #p<0.05. *Indicates death of mice, resulting in reduced mean mice weight values. F–H. The ratio of T_{EM}/effector T cells (F) and frequencies of $CD28^+$, $CD69^+$ (G), interferon-γ^+ and $Ki67^+$ (H) in the $CD8^+$ population of tumor and spleen with six treatment regimens. Mean±SEMs. Pairwise comparisons were performed. *p<0.05, **p<0.01, ***p<0.001. BLI, bioluminescence imaging; Ki-67, marker of proliferation Kiel 67; T_{EM}, effector memory T cell; PD-1, programmed cell death 1.

43 days) (figure 5A). Moreover, four of the nine long-term survivors in the D3 group displayed complete responses (figure 5D). Regarding the side effects of the combination, weight loss was generally less than 10%, and no significant differences were observed 3 days after the first treatment among the six treatment groups. Thereafter, the weight of the D3 group recovered faster than that of the other groups, indicating fewer side effects of the 3-day-delay combination (figure 5E).

Next, we elucidated the effects of sequential chemotherapy and PD-1 blockade therapy on immune functions. 3-day delay therapy appreciably increased the ratio of effector memory $CD8^+$ T cells to effector $CD8^+$ T cells in both the spleen and tumor tissues, indicating a shift in effector T cells toward an antigenic phenotype (figure 5F). Compared with the other treatments, systemic and tumor-infiltrating $CD8^+$ T cells were more activated, as evidenced by the increased expression of CD69 in the D3 group (figure 5G). Furthermore, intratumoral $CD8^+$ T cells exhibited increased proliferation and cytotoxicity (figure 5H). Collectively, these results demonstrate that a 3-day delay sequential therapy might be the optimal combination strategy for more effective antitumor activity.

The therapy with optimal combined timing results in a beneficial immune response in patients with NSCLC

Based on the data outlined above, we tested whether the combined timing or sequencing is appropriate for real-life clinical practice. As shown in figure 6A, 170 eligible participants with NSCLC were included in our real-world cohorts, including the control (combination, n=102) and experimental (3-day-delay sequential combination, n=68) cohorts. The comparable baseline characteristics between the two treatments allowed us to compare their efficacy and safety (online supplemental tables 1–3). To reduce the impact of potential confounders, we employed propensity score matching. A notable reduction in standardized mean difference after matching can be observed (online supplemental figure 4A), indicating that the propensity score matching effectively improved the balance of covariates between the two treatment groups. Careful inspection of the table shows that after propensity score matching, the p values of many covariates increase after matching (online supplemental table 2), and this change in p values confirms that our propensity score matching method successfully balances the distribution of baseline characteristics between the two groups. After propensity score matching, the matched cohort included 124 patients (online supplemental table 1). All 170 participants including 124 matched patients were prospectively observed, and the efficacy outcomes are summarized (figure 6B–D and online supplemental table 4). Remarkably, a large reduction in tumor mass in the lungs of several patients with NSCLC treated with a 3-day-delay sequential therapy (online supplemental figure 6) in the sequential cohort achieved a significantly higher ORR than that in the simultaneous cohort (67.74% vs 37.10%). Similarly, the disease control rate (DCR) in the sequential cohort (98.39%) was higher than that in the control cohort (80.64%) (figure 6C). Stratification of clinical responses demonstrated that markedly increased beneficial effects were observed in patients with a 3-day-delay in sequential therapy, but not in patients with simultaneous therapy (online supplemental figure 4B,C). We also observed that patients treated with sequential therapy had a longer median PFS (14.4 m vs 8.3 m, respectively, p=0.0013, figure 6D). Stratified studies of PFS demonstrated a significant increase in beneficial effects observed in patients with a 3-day delay in consecutive treatments (online supplemental figure 5A,B).

Subsequently, the underlying alterations in systemic immunity were studied using omics profiling. We performed TCR sequencing of the blood of 13 patients pretreatment and post-treatment (n=6, control group: Con; n=7, experimental group: Ex). Notably, the newly cloned T cells expanded effectively in the sequential cohort (median 81 (IQR 42–202)) versus 29 (IQR 17–78) in the simultaneous cohort at pre-Cycle3 (C3) therapy (D42) (figure 6E), which was consistent with the clinical efficacy outcomes (figure 6F). Simultaneously, three paired pretreatment and post-treatment PBMC from the simultaneous and sequential cohorts were randomly selected for bulk RNA-seq of $CD8^+$T cells. In both groups, longitudinal profiling of post-treatment (D7) $CD8^+$T cells revealed elevated effector function (Granzyme-B, IFN-γ), proliferation ability (Ki67), and activation phenotype (CD69) (figure 6G). This increase was more prominent in the sequential group than in the simultaneous group (figure 6G). GSEA results indicated that $CD8^+$T cells in the sequential group after 1 week of anti-PD-1 antibody treatment were inclined toward memory stem T cells (figure 6H). Flow cytometry was performed to observe the effect on $CD8^+$T cells in 24 patients (n=11, Con; n=13, Ex). Sequential therapy considerably increased the ratio of effector memory cells to effector $CD8^+$T cells (figure 6I). Patients in the sequential group also showed elevated $CD8^+$T cell activity, as IFN-γ and Ki67 expression increased (figure 6J). Together, these data support the hypothesis that 3-day-delay sequential therapy may be a better regimen in clinical practice.

DISCUSSION

Chemotherapy combined with anti-PD-1 antibody initially together is usually adopted in clinical practice and clinical trials.[6] Anti-PD-1 antibody have been reported to inhibit tumor growth by activating the immune system. Chemotherapy not only activates but also suppresses immune activity.[16 30] Therefore, it remains unclear whether simultaneous treatment is the best option in clinical practice.

We first used flow cytometry and RNA-seq to track dynamic changes in the immunity of patients with NSCLC and animal models after chemotherapy. The

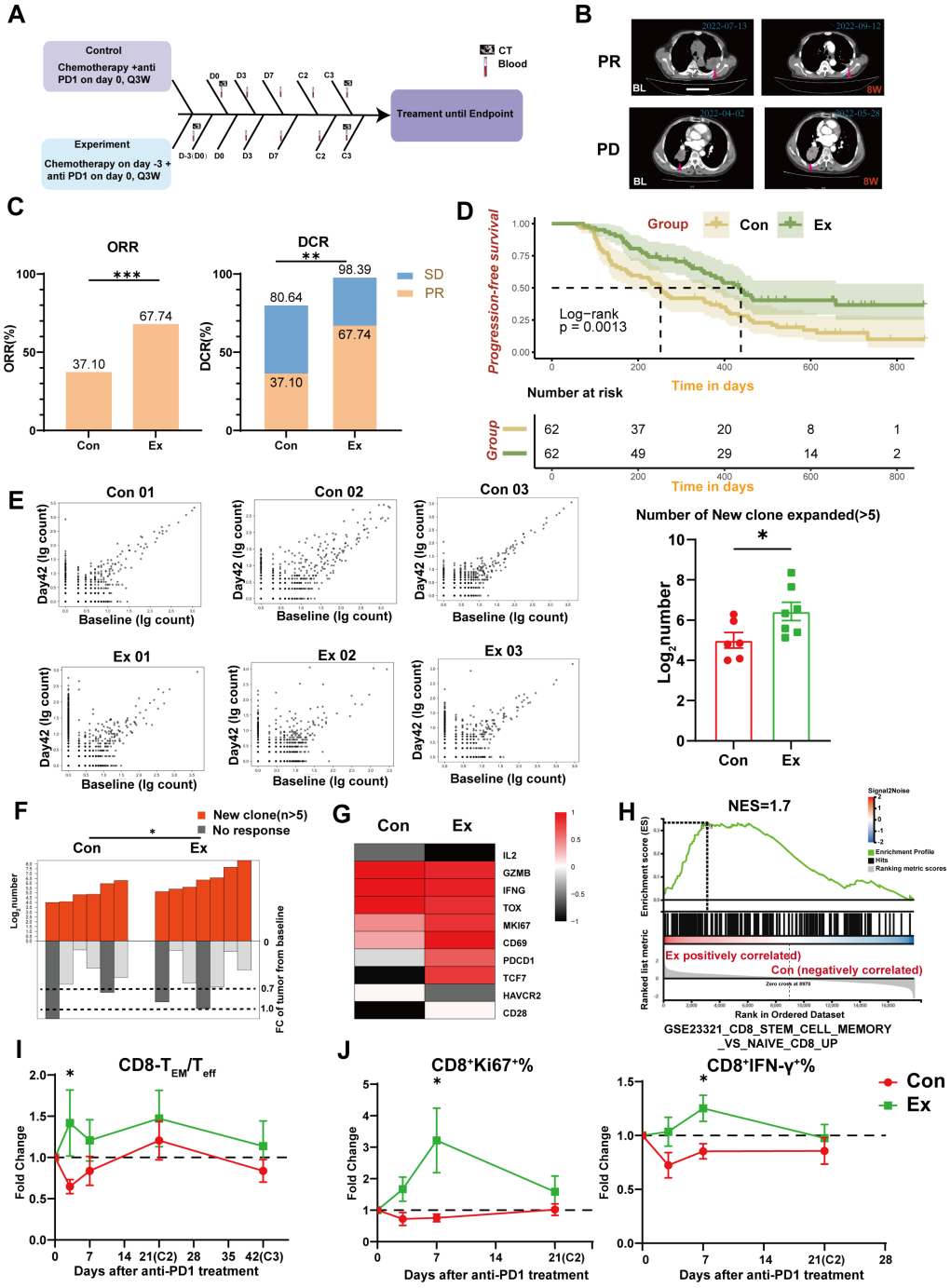

Figure 6 The chemo-anti-PD-1 combination with optimal timing results in a beneficial immune response in patients with NSCLC. (A) Schema showing the dosing schedule and relevant sample collection time points for each treatment group. (B) Examples of radiographic (CT scan) images of NSCLC pre-therapy and post-therapy. (C) The ORR and DCR were evaluated between the two groups after matching. (D) KM curves for progression-free survival of patients with NSCLC in two groups after matching (log-rank p value p=0.0013). (E). Scatter plots of the clone size of each clonotype in baseline (x-axis) and pre-C3 (day 42) (y-axis), with data of three patients summarized in each group. The number of new clones that occurred more than five times per patient after treatment, was counted. Mean±SEMs. Pairwise comparisons were performed. *p<0.05; Con, n=6; Ex, n=7. (F) SK plots included tumor maximum percentage change and a number of expanded new clones in both treatments. SK plots were created using an online software (https://skylineplotter.shinyapps.io/SkyLinePlotter/). (G) Heatmap showing transcriptome relative expression of key molecules in post-treatment (D7) compared with pretreatment (D0). (H) Gene Set Enrichment Analysis of memory stem T cells CD8 T cells signatures in D7 genes. (I–J) The ratio of T_{EM}/T_{eff} (I) and frequencies of interferon-γ^+ and Ki67$^+$ (J) in the CD8$^+$ population of two treatment regimens. Mean±SEMs. Pairwise comparisons were performed. *p<0.05. Con, control group; DCR, disease control rate; Ex, experimental group; Ki-67, marker of proliferation Kiel 67; KM, Kaplan-Meier; NES, normalized enrichment score; NSCLC, non-small cell lung cancer; ORR, objective response rate; PD, progressive disease; PR, partial response; PD-1, programmed cell death 1; Q3W, every 3 week; SD, stable disease; T_{eff}, effector T cells; T_{EM}, effector memory T cell;

results showed high levels of PD-1 and CD28 on $CD8^+$ T cells on D3. This may be attributed to $CD8^+$ T-cell activation mediated by the chemotherapy-induced immunogenic properties of tumor cell death[16 31] and the promotion of a beneficial response to PD-1 blockade.[13 21] The functional relevance of PD-1 expression during chronic antigen exposure is evident in the revival of T-cell function and concomitant control of viral loads or tumor burden following PD-1 antibody checkpoint blockade.[6 32 33] Furthermore, an elevated T_{CM}/T_{eff} ratio on D3 reflects the proliferation and differentiation potential of human T-cell subsets in response to homeostatic cytokines or antigen stimulation.[25] Meanwhile, transcriptome analysis showed that the migration and adhesion abilities were improved, which is beneficial for reaching the immune response site.[34]

Transcriptome sequencing revealed pathway enrichment for calcium influx on D3, and transcription factor enrichment analysis showed enrichment for RELA, with RELA ranking first in both sets of comparative results. Other studies have reported that calcium ions are known to serve as an important indicator for measuring T-cell activation.[35 36] RELA serves as a representative molecule for NF-κB activation.[37] This also shows the $CD8^+$ T cells' initial status of activation on D3. RELA is a subunit of the NF-κB transcription factor complex that translocates from the cell cytoplasm to the nucleus for gene transcription regulation on activation,[38] and NF-κB also acts as a transcription factor that binds to the promoters and enhancers of PDCD1.[39 40] Additionally, the p65 subunit may itself be phosphorylated, enhancing its transcriptional activity.[41] Thus, we showed that D3 is the optimal immune status for chemo-anti-PD-1 therapy.

We used ex vivo and in vivo experiments to verify the effects of sequential and simultaneous treatment on immunity and tumor growth. Anti-PD-1 antibody treatment on D3 showed the highest proportion of $Ki67^+$ and IFN-γ^+ cells in $CD8^+$ T and $PD\text{-}1^+CD8^+$ T cells, as well as the activated $CD28^+$ or $CD69^+$ cells, leading to considerable tumor inhibition. In accord with this, $CD8^+$ T cells in the blood after anti-PD-1 antibody therapy in patients with lung cancer were predominantly CD28-positive and were actively proliferating.[42 43] A 24-hour sequential immunotherapy regimen combined with low-dose chemotherapy may be effective for chemoimmunotherapy because it not only minimizes drug-related toxicity but also activates the tumor microenvironment.[8] Sequential combination treatment greatly increased the number of infiltrating cytotoxic T cells.[44] These results support our findings that a 3-day-delay sequential combination can improve antitumor activity more than other combinations in vivo and ex vivo.

Based on the aforementioned data, we conducted a multicenter observational prospective study to assess the safety and preliminary efficacy of sequential and simultaneous chemo-anti-PD-1 combination therapy. Patients in the sequential group showed an improved clinical response (ORR and DCR) with longer PFS and immune activation than those in the simultaneous group. In addition, patients in the sequential group demonstrated a more substantial expansion of new TCR clones in the peripheral blood 6 weeks after starting treatment, which matched the clinical response. In studies of anti-PD-1 antibody treatment for patients with melanoma and NSCLC, the expansion of T-cell clones consisted of novel clonotypes that had not previously been observed in the same tumor and further confirmed most of the new clonotypes in the post-treatment blood.[11 45] We speculate that this was due to the efficient expansion of nascent clones in T_{CM}-like cells.[46] Our conclusion was verified in a retrospective study of 12 patients with refractory lung cancer with the 3–5-day-delay sequential combination, but it was deficient in a prospective study and the underlying immune alteration.[10] Nevertheless, there was a lack of credibility because of the small sample size, and D2 after chemotherapy was not the optimal immune status for chemo-anti-PD-1 therapy compared with D3, which was proven in our data. In our study, we expanded the sample size and performed the first-in-human, multicenter, prospective clinical study on patients with advanced NSCLC. However, a longer follow-up period is required to clarify whether this translates to differences in long-term survival. The association of NF-κB signaling to T-cell functionality in response to anti-PD-1 treatment might only represent part of the full mechanism. In our transcription factor enrichment analysis of D3, in addition to RALA, FOXP1 and MYB are also significantly enriched, which have been reported to participate in T-cell phenotype and function.[47 48] The underlying molecular mechanisms need to be further elucidated in the future.

Considering that a 3-day-delay sequential combination achieves an appreciable synergistic clinical response and no obvious side effects compared with the traditional combination, this strategy has clinical potential for the development of universal antitumor therapies.

Data availability statement

Data used in the study are available from the corresponding author on reasonable request.

Author affiliations
[1]Biotherapy Center and Cancer Center, The First Affiliated Hospital of Zhengzhou University, Zhengzhou, Henan, China
[2]Department of Oncology, the First Affiliated Hospital of Zhengzhou University, Zhengzhou, Henan, China
[3]Department of Oncology, Henan Provincial People's Hospital, People's Hospital of Zhengzhou University, People's Hospital of Henan University, Zhengzhou, Henan, China
[4]Department of Respiratory and Critical Care Sleep Medicine, the First Affiliated Hospital of Zhengzhou University, Zhengzhou, Henan, China
[5]Department of Respiratory Medicine, The First Affiliated Hospital of Zhengzhou University, Zhengzhou, Henan, China

[6]Department of Oncology, the Second Affiliated Hospital of Zhengzhou University, Zhengzhou, Henan, China
[7]Cancer Center, Union Hospital, Tongji Medical College, Huazhong University of Science and Technology, Wuhan, Hubei, China
[8]Department of Tumor Immunotherapy, the Fourth Hospital of Hebei Medical University and Hebei Cancer Institute, Shijiazhuang, Hebei, China
[9]Department of Technology, Chengdu ExAb Biotechnology Ltd, Chengdu, Sichuan, China
[10]State Key Laboratory of Esophageal Cancer Prevention & Treatment, Zhengzhou, Henan, China
[11]School of Life Sciences, Zhengzhou University, Zhengzhou, Henan, China
[12]Tianjian Laboratory of Advanced Biomedical Sciences, Academy of Medical Sciences, Zhengzhou University, Zhengzhou, Henan, China
[13]School of Public Health, Zhengzhou University, Zhengzhou, Henan, China

Contributors YZ, YH and DW conceived the study. GQ provided scientific input during writing and interpretation of the study protocol. CZ and QL provided technical support for the construction of the animal models and in performing flow cytometry. SY, GQ and DW analyzed and interpreted clinical data. QZ directed and interpreted the bioinformatic analyses. YL and KG assisted in the collection of clinical specimens and patient information. YZ, LW, SY, YX, HL, HC, HW, FF, LM, SO, TS, NH, Li Liu, Lihua Liu, YD, WL and SC informed patients of treatment protocols and performed statistical analyses. ZZ provided technical support for T-cell receptor sequencing. The manuscript was written by YH, DW and GQ, in collaboration with all coauthors, and reviewed by YZ, who assured the accuracy of the reported data and adhered to the protocol. All authors have edited and approved the manuscript. YZ is responsible for the overall content as guarantor.

Funding This study was supported by grants from the International Science, Technology, and Innovation Cooperation Project of the State Key R&D Program (Grant No. 2022YFE0141000), the National Natural Science Foundation of China (Grant No. 82272873, 82473423, 82002564), and the Central Government of Henan Province Guides Local Science and Technology Development Fund Projects (Grant No. Z20221343036), and Science and Technology Project of Henan Province (Grant No. SBGJ202101010, SBGJ202003021, 232102311067, 222102310052, LHGJ20220050).

Competing interests None declared.

Patient consent for publication Not applicable.

Ethics approval This study involves human participants and was approved by the Ethics Committee of The First Affiliated Hospital of Zhengzhou University (ethics approval number: 2022-KY-0647-001). Participants gave informed consent to participate in the study before taking part.

Provenance and peer review Not commissioned; externally peer reviewed.

Data availability statement Data are available upon reasonable request. All data relevant to the study are included in the article or uploaded as supplementary information. Data used in the study are available from the corresponding author upon reasonable request.

ORCID iDs
Li Liu http://orcid.org/0000-0003-2314-8756
Lihua Liu http://orcid.org/0000-0002-1201-4624
Yi Zhang http://orcid.org/0000-0001-9861-4681

REFERENCES

1 Atkins MB, Plimack ER, Puzanov I, *et al*. Axitinib in combination with pembrolizumab in patients with advanced renal cell cancer: a non-randomised, open-label, dose-finding, and dose-expansion phase 1b trial. *Lancet Oncol* 2018;19:405–15.
2 Liu Z, Liu J, Li Z. Chemoimmunotherapy in advanced esophageal squamous cell carcinoma: optimizing chemotherapy regimens for immunotherapy combinations. *Sig Transduct Target Ther* 2022;7:233.
3 Ettinger DS, Wood DE, Aisner DL, *et al*. Non–Small Cell Lung Cancer, Version 3.2022, NCCN Clinical Practice Guidelines in Oncology. *J Natl Compr Canc Netw* 2022;20:497–530.
4 Grant MJ, Herbst RS, Goldberg SB. Selecting the optimal immunotherapy regimen in driver-negative metastatic NSCLC. *Nat Rev Clin Oncol* 2021;18:625–44.
5 Wu M, Huang Q, Xie Y, *et al*. Improvement of the anticancer efficacy of PD-1/PD-L1 blockade via combination therapy and PD-L1 regulation. *J Hematol Oncol* 2022;15:24.
6 Gandhi L, Rodríguez-Abreu D, Gadgeel S, *et al*. Pembrolizumab plus Chemotherapy in Metastatic Non-Small-Cell Lung Cancer. *N Engl J Med* 2018;378:2078–92.
7 Fu D, Wu J, Lai J, *et al*. T cell recruitment triggered by optimal dose platinum compounds contributes to the therapeutic efficacy of sequential PD-1 blockade in a mouse model of colon cancer. *Am J Cancer Res* 2020;10:473–90.
8 He X, Du Y, Wang Z, *et al*. Upfront dose-reduced chemotherapy synergizes with immunotherapy to optimize chemoimmunotherapy in squamous cell lung carcinoma. *J Immunother Cancer* 2020;8:e000807.
9 Xing W, Zhao L, Zheng Y, *et al*. The Sequence of Chemotherapy and Toripalimab Might Influence the Efficacy of Neoadjuvant Chemoimmunotherapy in Locally Advanced Esophageal Squamous Cell Cancer-A Phase II Study. *Front Immunol* 2021;12:772450.
10 Yao W, Zhao X, Gong Y, *et al*. Impact of the combined timing of PD-1/PD-L1 inhibitors and chemotherapy on the outcomes in patients with refractory lung cancer. *ESMO Open* 2021;6:100094.
11 Liu B, Hu X, Feng K, *et al*. Temporal single-cell tracing reveals clonal revival and expansion of precursor exhausted T cells during anti-PD-1 therapy in lung cancer. *Nat Cancer* 2022;3:108–21.
12 Wu TD, Madireddi S, de Almeida PE, *et al*. Peripheral T cell expansion predicts tumour infiltration and clinical response. *Nat New Biol* 2020;579:274–8.
13 Mazzaschi G, Facchinetti F, Missale G, *et al*. The circulating pool of functionally competent NK and CD8+ cells predicts the outcome of anti-PD1 treatment in advanced NSCLC. *Lung Cancer (Auckl)* 2019;127:153–63.
14 Luoma AM, Suo S, Wang Y, *et al*. Tissue-resident memory and circulating T cells are early responders to pre-surgical cancer immunotherapy. *Cell* 2022;185:2918–35.
15 Bezu L, Sauvat A, Humeau J, *et al*. eIF2α phosphorylation is pathognomonic for immunogenic cell death. *Cell Death Differ* 2018;25:1375–93.
16 Beyranvand Nejad E, van der Sluis TC, van Duikeren S, *et al*. Tumor Eradication by Cisplatin Is Sustained by CD80/86-Mediated Costimulation of CD8+ T Cells. *Cancer Res* 2016;76:6017–29.
17 Gao Q, Wang S, Li F, *et al*. High Mobility Group Protein B1 Decreases Surface Localization of PD-1 to Augment T-cell Activation. *Cancer Immunol Res* 2022;10:844–55.
18 Bally APR, Austin JW, Boss JM. Genetic and Epigenetic Regulation of PD-1 Expression. *J Immunol* 2016;196:2431–7.
19 Huang Q, Wu X, Wang Z, *et al*. The primordial differentiation of tumor-specific memory CD8$^+$ T cells as bona fide responders to PD-1/PD-L1 blockade in draining lymph nodes. *Cell* 2022;185:4049–66.
20 Boukhaled GM, Gadalla R, Elsaesser HJ, *et al*. Pre-encoded responsiveness to type I interferon in the peripheral immune system defines outcome of PD1 blockade therapy. *Nat Immunol* 2022;23:1273–83.
21 Duchemann B, Naigeon M, Auclin E, *et al*. CD8(+)PD-1(+) to CD4(+) PD-1(+) ratio (PERLS) is associated with prognosis of patients with advanced NSCLC treated with PD-(L)1 blockers. *J Immunother Cancer* 2022;10:e004012.
22 Pan Y, Fu Y, Zeng Y, *et al*. The key to immunotherapy: how to choose better therapeutic biomarkers for patients with non-small cell lung cancer. *Biomark Res* 2022;10:9.
23 Kwon M, An M, Klempner SJ, *et al*. Determinants of Response and Intrinsic Resistance to PD-1 Blockade in Microsatellite Instability-High Gastric Cancer. *Cancer Discov* 2021;11:2168–85.
24 Zhang Y, Chen H, Mo H, *et al*. Single-cell analyses reveal key immune cell subsets associated with response to PD-L1 blockade in triple-negative breast cancer. *Cancer Cell* 2021;39:1578–93.
25 Manjarrez-Orduño N, Menard LC, Kansal S, *et al*. Circulating T Cell Subpopulations Correlate With Immune Responses at the Tumor

Site and Clinical Response to PD1 Inhibition in Non-Small Cell Lung Cancer. *Front Immunol* 2018;9:1613.
26 Siddiqui I, Schaeuble K, Chennupati V, *et al*. Intratumoral Tcf1+PD-1+CD8+ T Cells with Stem-like Properties Promote Tumor Control in Response to Vaccination and Checkpoint Blockade Immunotherapy. *Immunity* 2019;50:195–211.
27 Burger ML, Cruz AM, Crossland GE, *et al*. Antigen dominance hierarchies shape TCF1^{+} progenitor CD8 T cell phenotypes in tumors. *Cell* 2021;184:4996–5014.
28 Legut M, Gajic Z, Guarino M, *et al*. A genome-scale screen for synthetic drivers of T cell proliferation. *Nature New Biol* 2022;603:728–35.
29 Gros A, Tran E, Parkhurst MR, *et al*. Recognition of human gastrointestinal cancer neoantigens by circulating PD-1+ lymphocytes. *J Clin Invest* 2019;129:4992–5004.
30 Zhang F, Li R, Yang Y, *et al*. Specific Decrease in B-Cell-Derived Extracellular Vesicles Enhances Post-Chemotherapeutic CD8^{+} T Cell Responses. *Immunity* 2019;50:738–50.
31 Nunès JA, Olive D. CD28 costimulation promotes an antitumor CD8+ T cell response in myeloid antigen-presenting cell niches. *Cell Mol Immunol* 2022;19:147–9.
32 Barber DL, Wherry EJ, Masopust D, *et al*. Restoring function in exhausted CD8 T cells during chronic viral infection. *Nature New Biol* 2006;439:682–7.
33 Paz-Ares L, Luft A, Vicente D, *et al*. Pembrolizumab plus Chemotherapy for Squamous Non-Small-Cell Lung Cancer. *N Engl J Med* 2018;379:2040–51.
34 Laidlaw BJ, Zhang N, Marshall HD, *et al*. CD4+ T cell help guides formation of CD103+ lung-resident memory CD8+ T cells during influenza viral infection. *Immunity* 2014;41:633–45.
35 Feske S. Calcium signalling in lymphocyte activation and disease. *Nat Rev Immunol* 2007;7:690–702.
36 Ping Y, Shan J, Qin H, *et al*. PD-1 signaling limits expression of phospholipid phosphatase 1 and promotes intratumoral CD8^{+} T cell ferroptosis. *Immunity* 2024;57:2122–39.
37 Thompson JE, Phillips RJ, Erdjument-Bromage H, *et al*. I kappa B-beta regulates the persistent response in a biphasic activation of NF-kappa B. *Cell* 1995;80:573–82.
38 Perkins ND. Integrating cell-signalling pathways with NF-kappaB and IKK function. *Nat Rev Mol Cell Biol* 2007;8:49–62.
39 Pichler AC, Carrié N, Cuisinier M, *et al*. TCR-independent CD137 (4-1BB) signaling promotes CD8^{+}-exhausted T cell proliferation and terminal differentiation. *Immunity* 2023;56:1631–48.
40 Chamoto K, Yaguchi T, Tajima M, *et al*. Insights from a 30-year journey: function, regulation and therapeutic modulation of PD1. *Nat Rev Immunol* 2023;23:682–95.
41 Duran A, Diaz-Meco MT, Moscat J. Essential role of RelA Ser311 phosphorylation by zetaPKC in NF-kappaB transcriptional activation. *EMBO J* 2003;22:3910–8.
42 Kamphorst AO, Wieland A, Nasti T, *et al*. Rescue of exhausted CD8 T cells by PD-1-targeted therapies is CD28-dependent. *Science* 2017;355:1423–7.
43 Kamphorst AO, Pillai RN, Yang S, *et al*. Proliferation of PD-1+ CD8 T cells in peripheral blood after PD-1-targeted therapy in lung cancer patients. *Proc Natl Acad Sci U S A* 2017;114:4993–8.
44 Zhu C, Shi Y, Li Q, *et al*. Rational administration sequencing of immunochemotherapy elicits powerful anti-tumor effect. *J Control Release* 2022;341:769–81.
45 Yost KE, Satpathy AT, Wells DK, *et al*. Clonal replacement of tumor-specific T cells following PD-1 blockade. *Nat Med* 2019;25:1251–9.
46 Grassmann S, Mihatsch L, Mir J, *et al*. Early emergence of T central memory precursors programs clonal dominance during chronic viral infection. *Nat Immunol* 2020;21:1563–73.
47 Tsui C, Kretschmer L, Rapelius S, *et al*. MYB orchestrates T cell exhaustion and response to checkpoint inhibition. *Nature New Biol* 2022;609:354–60.
48 Zhu Z, Lou G, Teng X-L, *et al*. FOXP1 and KLF2 reciprocally regulate checkpoints of stem-like to effector transition in CAR T cells. *Nat Immunol* 2024;25:117–28.